

Diagnosis of ECG Signal for Signal Quality Using Convolutional Neural Networks

A.RAJANI¹, M .GAYATHRI²

¹Assistant Professor, ECE, JNTUK, Kakinada, India

²Student, M.Tech, ECE, JNTUK, Kakinada, India

Abstract -In this paper, we propose a new automated quality- alert electrocardiogram (ECG) beat categorization method for effective analysis of ECG arrhythmias under unverified healthcare environments. The existed technique consists of three major stages: 1) the ECG signal quality assessment ("accept- able" or "unacceptable") based on our earlier customized complete ensemble empirical mode decaying and temporal features; 2) the ECG signal reformation and R-peak recognition; and 3) the ECG beat categorization as well as the ECG beat extraction, beat arrangement, and normalized cross-correlation-based beat categorization. The exactness and robustness of the existing method are evaluated using dissimilar normal and abnormal ECG signals taken from the standard MIT-BIH arrhythmia beat categorization method can significantly achieve false alarm reduction ranging from 24% to 93% under noisy ECG recordings. The R-peak detector achieves the average Se 99.67% and positive predictivity (Pp) 93.10% and the average sensitivity (Se) 99.65% and Pp 98.88% without and with denoising approaches, correspondingly. Results further showed that the proposed ECG beat extraction approach can improve the categorization accuracy by using CNN technique for categorization .By using CNN technique the results were better as the R-peak detection achieves the average Se=99.67% and Pp=93.10% and the average Se=99.65% and Pp=98.88%,without and with denoising approaches, respectively. with the SQA approach, the R-peak detector achieves the average Se=99.86% and Pp=99.84%.It shows that the proposed technique improves the consistency with improved categorization accuracy and F1 score. database assessment results show that the proposed quality- aware ECG

Key Words: ECG beat classification, ECG arrhythmia recognition ,signal Quality assessment, Convolutional neural networks.

1.INTRODUCTION

Accurate and steady classification of electrocardiogram (ECG) beats is influential in automatic ECG diagnosis uses under resting, exercise and ambulatory ECG footage circumstances [1]–[8]. Some process have been offered with various signal processing methods and classifiers.

Table 1 review the workings of the presented ECG beat classification techniques. The ECG beat classification method usually consists of three key steps: (i) preprocessing, (ii) feature extraction, and (iii) classification.

1.1 Accessible ECG Beat Classification Methods

The preprocessing stage is usually designed to block out backdrop noises by the denoising methods as the two median filters [4]–[7], highpass filter (HPF) with cut-off frequency of 1 Hz [8], bandpass filter with 0.1-100 Hz [9], morphological filtering [10], multiscale principal component analysis (MSPCA) [11], wavelet trans-form [12], [13], band-pass filtering with 5-12 Hz [12] for removal of baseline wanders; second order Butterworth low- pass filter (LPF) with 30-Hz cutoff frequency [8], bandpass filtering [9], [12], 12-tap LPF [4], MSPCA filtering [11], morphological filtering [10], and notch filter [8]. In the past methods, different signal processing techniques were proposed for extracting the features from ECG signals. The features are: temporal morphological features [4], [12], [14], frequency domain features, wavelet morphological features, Stockwell transform (ST) features [9], Hermite coefficient features [15], [16], statistical features (time-domain, frequency-domain and time-frequency domain) [11], RR interval features [12], wavelet cross spectrum (WCS) and wavelet coherence (WCOH) features [13] and independent component analysis (ICA) [17]. Based on the extracted features, the beat classification was performed using the linear discriminant analysis (LDA) [4], neural network [18], neuro-fuzzy network [15], rule-based rough sets [14], geometric template matching [19], block- based neural networks (BbNNs) [16], support vector machine (SVM) [12], particle swarm optimization (PSO) [20], multidimensional PSO (MD PSO) based multilayer perceptrons (MLPs) [21], hidden Markov models [22], mixture of experts with self organizing maps (SOM) and learning vector quantization (LVQ) algorithms [24], random forests (RF) classifier [11], extreme learning machine (ELM) [10] and 1-D convolutional neural networks (CNNs) [23]. S. Kiranyaz et al. proposed patient-specific ECG beat classification approach based on the beat detection, the raw ECG morphology wave- form, beat timing information and adaptive 1-D convolutional neural networks (CNNs) [23].

Table -1: REVIEW OF THE EXISTING ECG BEAT CLASSIFICATION METHODS

Ref.	Preprocessing	ECG Features	Classifier	Database (Lead)	Beat Classes	Accuracy (%)
Chazal [4]	MF, LPF	Morphology, RR	LD	MITDB (I)	N,S,V,F,Q	80.61
Chazal [5]	MF, LPF	Morphology, RR	LD	MITDB(I)	N,S,V,F,Q	95.7
Mar [6]	MF, LPF	Temporal, Morphological, Statistical	MLP, LDA	MITDB(I)	N,S,V,F	89
Lin [7]	MF, LPF	Morphology+RR	LD	MITDB(I)	N, S, or V	86
Li [8]	HPF	Spectral, Temporal, Statistical	SVM	AHADB,CUVTD, MITMVAD	VTVF	98.23
Das [9]	BPF	RR, S- transform, BFO	SVM	MITDB(I)	N, V, S, F, Q	98.4
Kim [10]	MoF	CWT, Morphology, RR,PCA, LDA	ELM	MITDB(I)	N,S,V,F,Q	97.94
Alekovic [11]	DWT, PCA	Statistical features	CART, C4.5, RF	MITDB(I), INCARTDB (12)	N, LBBB, RBBB, APC, PVC	99.33
Ye [12]	Wavelet	Wavelet,ICA,RR	SVM	MITDB(II)	N,L,R,A,P,V,F,V,F,a,f,e,E,j,Q,x	99.3
Banerjee [13]	DWT	Cross Wavelet, WCS, WCOH	Threshold	ptbdb(12)	inferior myocardial infarction	97.60
Mitra [14]	CEPP	Morphology	Rough Set	Real-Time (12)	N,A, B,T,E,D,I,M	100 (N), 95.8(I),100(M)
Linh [15]	-	Hermite Polynomial	Neuro-Fuzzy	MITDB	V, L, R, A, I, E	96
Jiang [16]	-	Hermite,RR	BNN	MITDB	N,S,V,F,Q	98.1(V), 96.6(S)
Saez [19]	-	Polynomial, GA	GM	MITDB(I)	N,L,R,A,P,V,F,a,f,E,j,Q,x	93.98
Melgani [20]	-	Morphology, Temporal,RR	SVM,PSO	MITDB	N,A,V,R,L,P	89.72
Ince [21]	DWT	Wavelet,RR	EANN	MITDB(I)	N,S,V,F,Q	98.3(V),97.4(S)
Hu [24]	-	Morphology, Temporal	SOMMLVQ	MITDB(I)	N,V,F,Q	82.6
Kiranyaz [25]	-	Temporal,Spectral	CNN	MITDB(I)	N,S,V,F,Q	99 (V), 97.6 (S)

Note:MF,Median Filters;LPF low pass filter,GM,Geometric Matching;WCS,Wavelet Cross Spectrum,WCOH,Wavelet coherence,ptbdb,st-petersburg Institute of cardiological Technics 12-lead,Arrhythmia Database;MoF,Morphological filtering,BFO,Bacteria Foraging Optimization algorithm.LD, Linear Discriminant, CEPP, Cool Edit Pro package; AHADB, American Heart Association Database; CUVTD,Creightoa University Ventricular Tachyarrhythmia Database, MITVAD, MIT-BIH Malignant Ventricular Arrhythmia Database; BbNN,Block-based neural Network; CNN,convolutional Neural Networks, SOM, self-Organization Map; LVQ ,Learning vector Quantization; ELM. Extreme Learning Machine; MLP, Multi-Layer perceptron; SVM, Support Vector Machine; PSO, Praticie swarm optimization;PCA,Principial Component Analysis;ICA, Independent Component Analysis;MI Myocardial Infarction; DWT, Discrete Wavelet Transformation; BPF, Band pass Filter;GA, Genetic Algorithm, EANN,Evolutionary Artificial NN.

The authors observed that there is a significant variation in the system’s accuracy and reliability for the larger databases and noisy ECG signals with physiological artefacts and external noises.

1.2 Related Works and Motivation

Extraction of accurate morphological features plays a vital role in most aforesaid ECG beat classification methods. Literature studies verified that the précised determination of R-peaks, ECG beat taking out, and ECG morphological characteristic taking out is still a difficult job in the existence of diverse nature of artifacts and noises as well as as well as baseline wander (BW), abrupt change (ABC), flat line (FL), power line interference (PLI), muscle artifacts (MA) and instrument noise (IN) [25], [26]. The existence of the noises guide to more false alarms due to the extent of noisy feature parameters. Hence, the preprocessing stage of the existing most process employed denoising technique(s) to decrease the effect of the aforesaid noise sources. Even though the denoising techniques are able of restrain the artifacts and noises, the denoising method change the morphological outline of the confined waves of both noise-free and noisy ECG signals. The heartbeat waveform modification can guide to wrong analysis of ECG arrhythmias due to the misclassification of the ECG beats.

Thus, an automatic quality assessment of ECG signals can able of dropping false alarm rates and misclassification rates. Many endeavors have been made for fine and ranking the excellence of the ECG signals [27]–[29]. A few of the accessible ECG signal quality assessment (SQA) methods based on the diverse removed features from single and 12-leads (I, II, III, aVR, aVL, aVF, V1, V2, V3, V4, V5, and V6) ECGs are for a short time reviewed in the next section.

1.3 ECG Signal Quality Assessment Algorithms

The ECG signal excellence assessment (ECG-SQA) plays a main vital role in consistent heart rate variability (HRV) analysis, unsupervised telehealth monitoring, emotional recognition and biometric authentication [26], [29]. Accessible ECG-SQA process were based on the linear signal subspace scrutiny with supervised machine learning [27], RR-interval features with heuristic system and template identical [30], modulation spectral signal manageable [28], steadiness of PQRST complexes [31], with features like relative baseline and QRS complex sub-band power, higher order statistics (skewness and kurtosis) and five important components along with support vector machine (SVM) classifier [29], [32], [33], empirical mode decomposition and statistical approaches [34], QRS complex and RR interval-based elements [35], multichannel adaptive filtering [36], time-domain features for instance amplitude, slope, etc., [37], [38], using features like crossing points among distinctive leads, and relative magnitude of QRS complex and noise [39], [40], linear prediction error [41], a set of rules [42], kurtosis with ECG spectral distribution and Kalman filter [29], and modified complete ensemble empirical mode decomposition and temporal features [43]. Most aforesaid methods include two major steps: heartbeat feature extraction and signal quality grading. For computing the signal quality indexes (SQIs), different time-domain and spectral features, RR-interval and QRS complex-based features, higher-order statistical features are extracted from the processed ECG signal [27]–[43]. Some of the techniques used a set of assessment rules and machine learning come up to categorize the recorded ECG signals into two-four quality collections such as acceptable and unacceptable; acceptable, intermediate and unacceptable; and excellent, very good, good and bad [43] based on the exact SQI values. The restrictions of most techniques is the exact and consistent taking out of the ECG morphological features that can be extremely complicated under time-varying ECG morphological outlines and heart rates [43].

1.4 Contribution of this Paper

In this paper, we present a quality-aware ECG beat classification process for unsupervised ECG monitoring applications. It consists of three major stages: (i) the ECG signal quality assessment (ECG-SQA) (“acceptable” or “unacceptable”) based on our earlier modified complete ensemble empirical mode decomposition (CEEMD) and temporal features, (ii) the ECG signal restoration and R-peak

recognition and (iii) the ECG beat categorization including the ECG beat extraction, beat alignment and normalized cross-correlation (NCC) based beat classification. The ECG signal quality assessment was applied based on the modified CEEMD algorithm and temporal features such as number of zerocrossings (NZC), maximum absolute amplitude (MAA), and short-term NZC envelope as described in our earlier work [43]. In the next stage, the acceptable ECG signals are additional procedure for classifying the ECG beats present in the ECG signal. In the third stage, the heartbeat classification is executed by the NCC based waveform resemblance metric score which is intended among a test heartbeat model and the reference models that are accumulated in the heartbeat database.

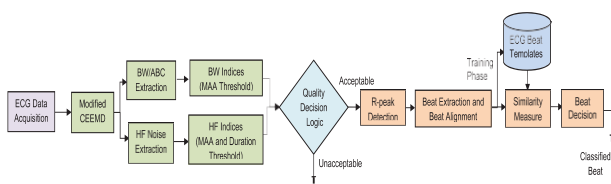


Fig -1: Block diagram of the existed quality-aware heartbeat classifier.

The rest of this paper is organized as follows. Section 2 describes the existed quality-aware heartbeat categorization method. The ECG signal quality evaluation is presented for reviewing the ECG signal quality. The ECG denoising approach is presented for conserving the QRS complex morphology as hold back the backdrop noises. The noise- vigorous R-peak recognition approach is accessible for extracting the ECG beats. A uncomplicated waveform comparison based approach is presented for ECG beat classification. Section 3 presents the presentation of the ECG beat categorization methods assess using the standard ECG databases in diverse variety of noises. Also, the false alarm reduction (FAR) development is presented. Finally, conclusions are drawn in Section 4.

2. Existed Quality-Aware ECG Beat Classifier

A basic block diagram of the existed quality-aware ECG beat categorization technique is demonstrate in Fig. 1 which consists of five steps: modified CEEMD based ECG decomposition, the CEEMD based ECG signal quality assessment, the collective R-peak finding and ECG improvement, R-peak arrangement and the ECG beat removal and the beat similarity identical. These steps are explained in the next subsections

2.1 Customized CEEMD Based ECG Decomposition

In this examine, the CEEMD is used for decompose of the ECG signals as an choice of the EMD and ensemble EMD algorithms since of two reasons: (i) the mode mixing problem of the fundamental EMD, where dissimilar oscillations be in the same IMF, or similar oscillations be in unlike IMFs; and (ii) the ensemble EMD (EEMD) produce unreliable number of IMFs [48]. Torres et al. proposed the

CEEMD algorithm that inserts dissimilar awareness of Gaussian noise to the remaining signal after removeing successive intrinsic mode functions [48]. It was confirmed that the CEEMD algorithm gives the exact rebuilding of the signal and an enhanced spectral partition of the modes, with a lower computational cost by needs less than half the sifting iterations as compared to that of the EEMD algorithm.

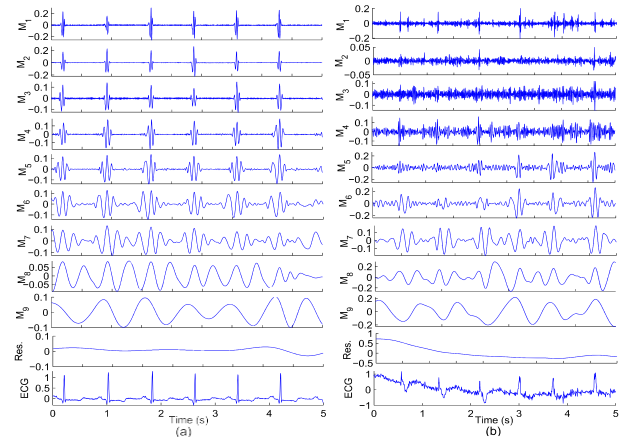


Fig - 2: Demonstrate the IMFs obtained using the modified CEEMD algorithm for the (a) Noise-free ECG signal, and (b) Noisy ECG signal with baseline wanders and muscle artifacts

The compensation of modified CEEMD with noise-specific stopping criteria were explored in our earlier works [43]. The existed stopping criteria is based on number of zerocrossings (NZC) and utmost maximum amplitude (MAA) to find the baseline wanders and to know its severity in the deposit signal. This stopping criterion can ease the computational load by stopping the additional decomposition which may not be necessary for analysing the ECG components [43]. The breakdown results of the modified CEEMD algorithm are illustrated in Fig. 2. It is noted that the first one or two IMFs (labelled as M_1 and M_2) capture fast varying components including MA, PLI and Gaussian noise and high frequency (HF) components of QRS complexes. In the meantime, other IMFs capture the ECG components including low- frequency (LF) parts of the QRS complex and the P and T waves. It is additional noted that the baseline wander is captured in the deposit by using the proposed stopping criteria.

2.2 ECG Signal Quality Assessment

In this study, the quality assessment of the ECG signals is performed based on our previous work [43]. For signal quality assessment, the decomposed IMFs are cluster into the HF sub-signals including the MA, PLI, IN and HF components of QRS complexes, the LF signal as well as baseline wanders, and the ECG signal with the local waves such as P-wave, QRS-complex and T-wave. Fig. 3 (a) and (b) shows the reconstructed aforesaid sub-signals of the 5 s ECG signal. The baseline wander is apprehended by the rest gained using modified CEEMD algorithm that is

shown in Fig. 3 (a(ii)) and (b(ii)). The ECG signal corrupted with both BW and unexpected change is shown in Fig. 4 (b). It is noted that the sudden change disturbance causes the sudden amplitude

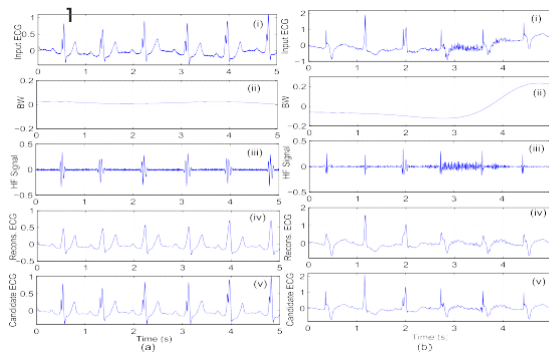


Fig - 3: Illustrates the sub-signals of the original ECGs

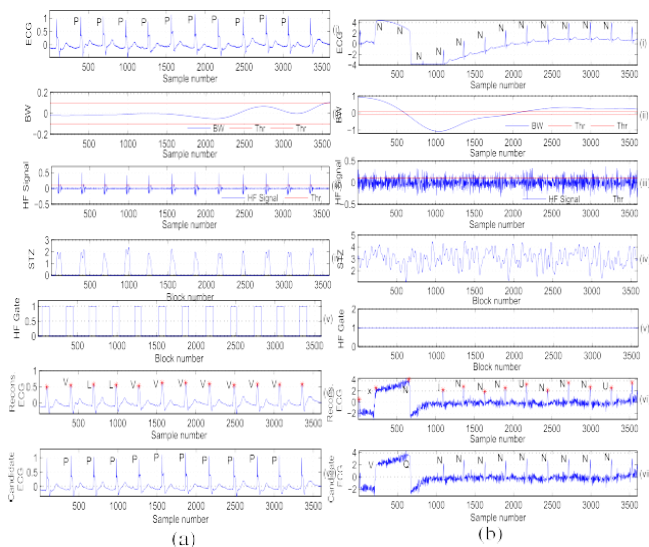


Fig - 4: Illustrates the effectiveness of the proposed SQA approach in detecting the signal quality with performance improvement in beat classification for clean ECG signal and the presence of the abrupt change in the ECG signal.(a) Noise-free ECG signal. (b) ECG plus abrupt change.

Differences in the remains as shown in Fig. 4 (b(ii)). Based on our explanations, a global thresholding of 0.2 mV and limited MAA thresholding of 0.1 mV are used to sense the occurrence of the sudden amplitude difference. For now, the BW can be efficiently detached by the heartbeat waveform removal. However, sudden amplitude variation can deform the morphological shapes of the signal while suppressing the sudden components. Thus, the ECG signal segments corrupted with sudden change are measured as Unacceptable. It is noted from Figs. 2, 3 that the HF noises such as MA, PLI, IN are adequately detained in initial three IMFs. Also, high frequency components of the QRS complex are also detained in the first few IMFs. To analyses the severity of the HF noises, the signal is created by adding the first three IMFs as follows:

$$h[n] = \sum_{i=1}^3 IMF_i[n] \quad (1)$$

where, h (n) is the created HF signal. Figs. 5 (a(iii)), (b(iii)) show the recreated HF signal for an ECG signal tainted with MA and PLI waveforms. Figs. 5 (a(iii)), (b(iii)) show that the recreated HF signals sufficiently confine the MA, PLI and the HF information of QRS complexes. For now, Fig. 4(a(iii)) shows that the contained HF components of the QRS complexes are conquered in case of the noise-free ECG signals. Further, Fig. 4 (b(vi)) shows that taking away of HF noises can change the shape of the heartbeat waveform that can direct to false classification of heart beats.

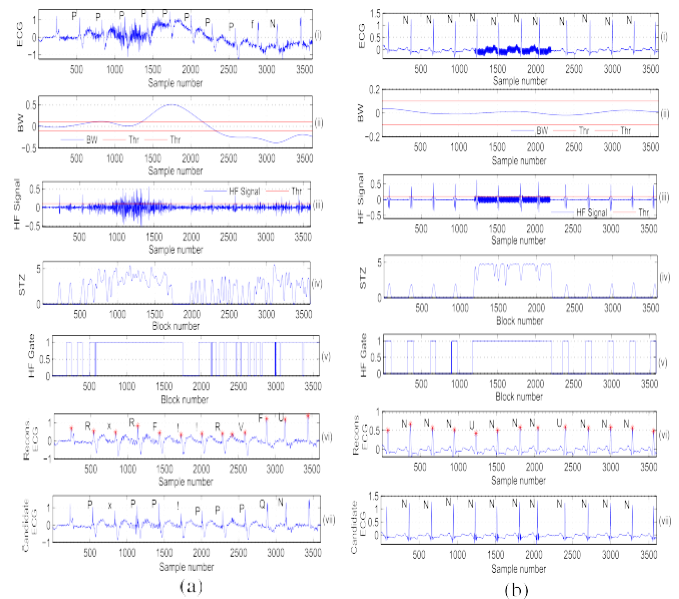


Fig - 5: Illustrates the effectiveness of the proposed SQA approach in detecting the signal quality with performance improvement in beat classification for ECG signal with BW and MA and the ECG signal with localized PLI (a) ECG plus BW and MA. (b) ECG plus PLI.

For sensing the occurrence of HF noises, smoothed mark envelopes of short-term zerocrossing (STZ) are removed and shown in Fig. 4(a(iv)) for noise-free ECG signal and Figs. 4(b(iv)), 5(a(iv)) and 5(b(iv)) for noisy ECG signals. Fig. 4(a(iv)) shows that the STZ mark envelope is composed of localized short interval pulses at the QRS complex areas and nil values in the low-amplitude noise sections for the noise-free ECG signals. For now, the STZ mark envelopes of the Figs. 4(b(iv)), 5(a(iv)) and 5(b(iv)) show the false peaks with wider duration for the ECG signals tainted with HF noises. Thus, the gate signal can be calculated as

$$g[n] = \begin{cases} 1, & STZ[n] > 0 \\ 0, & \text{Otherwise.} \end{cases} \quad (2)$$

The gate signals are shown in Fig. 4(a(v)) for noise-free ECG signal and Figs. 4(b(v)), 5(a(v)) and 5(b(v)) for the noisy ECG signals. In this study, the maximum absolute amplitude (MAA), short-term zerocrossing (STZ) and gate width duration features are used for the categorizing the signal into acceptable and unacceptable quality. The acceptable excellence signals are additional processed for categorization of heartbeats.

2.3 Combined R-Peak Detection and ECG Signal Enhancement

The conservation of the QRS complex segments is most important for accurate classification of different shapes of the ECG beats. In this examine, we contemporary the ECG denoising approach with instantaneous QRS complex conservation and background noise suppression. The recreated ECG is obtained by summing all the IMFs except the first three IMFs,

$$y[n] = \sum_{k=4}^I IMF_k[n] \tag{3}$$

where $y[n]$ is the recreated ECG signal and I is the totality number of IMFs. As the first three IMFs and rest are barred, the recreated signal is free from the baseline wanders and some of HF noises. The restructured signals lead to misclassification of the heartbeats. Consequently, this study are shown in Fig. 4(a(vi)) for the noise-free ECG signal and Figs. 4(b(vi)), 5(a(vi)) and 5(b(vi)) for the noisy ECG signals. It is observed that the HF components of the QRS complexes are not potted by this reformation process. Results of the Fig. 4 (a(vi)), (b(vi)) and Fig. 5 (a(vi)), (b(vi)) express that the QRS complex shape difference can focuses on the conservation of the QRS complex portion by giving out the localized residual components that are present in the first three IMFs. Here, the applicant ECG signal is created by adding reconstructed ECG signals $y(n)$ and the removed HF portions of QRS complex from the HF signal $h(n)$ within the duration of 100 ms centered at the sensed R-peak instants [44]. The R-peak finding is executed using the algorithm accessible in [45], which does not use any search-back rules with sets of finding thresholds and learning phase dissimilar other presented R-peak finding algorithms. For the detected R-peak time instantaneous as given by (n_1, n_2, \dots, n_K) , the HF component

of the QRS complex is given by

$$q_{HF}[n] = \begin{cases} h[n], & \text{for } n_i - P/2 \leq n \leq n_i + P/2 \\ 0, & \text{Otherwise} \end{cases} \tag{4}$$

where P corresponds to the block size of 100 ms. The candidate ECG signal is constructed as

$$z[n] = y[n] + q_{HF}[n] \tag{5}$$

The reconstruction results of this procedure are shown in Fig. 4 (a(vii)), (b(vii)) and Fig. 5 (a(vii)), (b(vii)). Results show that the planned denoising approach can capable of conserveing the HF portions of the QRS complexes. Finally,

the heartbeats are removed from the recreated ECG signal using the detected R-peaks [26]. The pseudocodes of the R-peak finding and heartbeat extraction approaches are described in Algorithm 1.

2.4 R-Peak Alignment and ECG Beat Extraction

The significance of the R-peak arrangement process is illustrated in Fig. 6. Fig. 6(a) and (b) show the removed ECG beats from the two types of ECG signals and the collection of the removed ECG beats without using the R-peak arrangement process, respectively. Fig. 6(c) and (d) show the removed ECG beats from the two types of ECG signals and the collection of the removed ECG beats with the R-peak alignment process. Some of the removed ECG beat templates are shown in Fig. 7. These templates were stored in the ECG beat template database for categorize the heartbeats present in the ECG signal during the testing segment.

Algorithm 1: R-Peak finding and Heartbeat Template taking out Algorithm

Function: $[R_{peak}, ECG\ Beat] = R_{peak}\ ECG\ beat\ Extraction$

(x, F_s)

Input: $x[n]$:= Input ECG signal; $n = 1, 2, \dots, N$

Output: $R_{peak}[n_k]$:= identified R-peak instants in ECG signal

Procedure

Step 0: Use Gaussian window for band pass filtering and compute first order difference

$$h[p] = G[p] - G[p - 1]; G = e^{-\frac{1}{2}(\frac{2\pi f}{L})^2}$$

$tt[n] := \text{filtfilt}(h, 1, x)$; //zero phase filtering

$d[n] := tt[n + 1] - tt[n]$

Step1: Apply adaptive thresholding,

$\tilde{d}[n] = (|d[n]|^2 > \sigma_d) * |d[n]|^2$, σ_d corresponds to the standard deviation of $d[n]$.

$b = \text{ones}(1, W)/W$; and $a = 1$; $W = [2.5 * F_s]$

Step 3: Peak detection using Gaussian derivative operator

$z[n] = s * h$ //convolution of $s[k]$ and $h[k]$

$rp = (\text{sign}(z[n]) > 0) \&\& (\text{sign}(z[n + 1]) < 0)$;

// store locations of negative zero-crossing points in $z[n]$

Step 4: R Peak location correction $wsz = [0.05 * F_s]$ // window size to search true R-peaks

for $k = 1$ to $\text{length}(rp)$ **do**

$[Rpeak] = \max\{x[rp(k) - wsz : rp(k) + wsz]\}$ //store corrected locations

Endfor

Step 5: ECG Beat Extraction and Template Creation

for $i = 1$ to $n_k - 1$;

Read ECG beat: $s1[m] = s[Rpeak[i] : Rpeak[i + 1]]$; $m = 1, 2, \dots, M$,

Left shifting: $s2[m] = s1[Rpeak[i] - shift : Rpeak[i + 1] - shift]$,

Peak aligning by circular shifting: $s3[m] = \tilde{s2}[m - shift - 1]_M$,

where, $\tilde{s}_2 [m]M$ is considered as a circular sequence of length M ,

Perform period normalization: $s4[l] = \text{interpft}(s3, L)$,
 //interpolation in FFT domain

Perform amplitude normalization: $s5[l] = s4[l]/|\max(s4[l])|$,

Perform peak centering: $s6[l] = \text{fftshift}(s5[l])$,

Construct ECG beat matrix: $b[i,:]= s6[l]$,

End.

Perform the ensemble averaging of all the same beat types (Let p type) for template creation as

$$T_p = \frac{1}{n_k} \sum_{k=1}^{n_k} b(k, :)$$

End

2.5 ECG Beat Classification

In this study, we assess the future quality-aware ECG beat categorization method for recognizing the normal beat (N), ventricular ectopic beat (V), supra ventricular ectopic beat (S), and paced beat (P) using the standardized cross-correlation measure between the reference heartbeat templates and the test heartbeat template. The heartbeat similarity is measured as

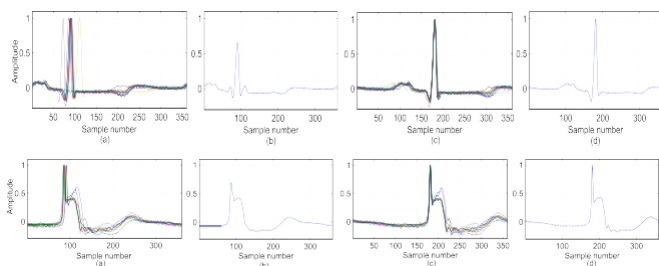


Fig - 6: Illustrates the significance of the R-peak alignment for ECG beat template creation. (a) Extracted ECG beats without R-peak alignment the extracted ECG beats as shown in (a); (c) Extracted ECG beats with R-peak alignment; and (d) Ensemble of the R-peak aligned extracted ECG beats as shown in (c) for the two types of ECG signals.

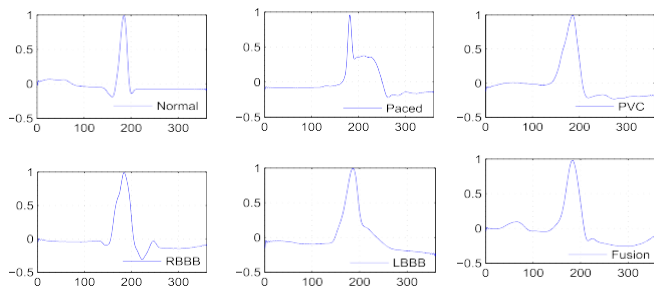


Fig - 7: Examples of reference templates for different ECG beats.

$$\Gamma = \frac{\sum_{m=1}^M [b_m(k) - \mu_0] \sum_{p=1}^P [T_p(k) - \mu_1]}{\sqrt{\sum_{m=1}^M [b_m(k) - \mu_0]^2} \sqrt{\sum_{p=1}^P [T_p(k) - \mu_1]^2}} \quad (6)$$

where, Γ represents the likeness measure, b_m is m th ECG beat, P is the number of classes of heartbeat types, M is the number of heartbeats and μ_0, μ_1 are the mean of the m th heartbeat b_m and template T_p , respectively. Based on the RR-interval and Γ values, the test heartbeats are classified into different heartbeat classes. The pseudocode of the proposed quality-aware heartbeat classification method is afforded in Algorithm 2. Consequences of this stage are shown in Figs. 4 (a(vii)), 5 (b(vii)). It can be seen that the heartbeats are suitably classified by using the recreated ECG signal. It is noted that heartbeats are not correctly classified in presence of severe muscle artifacts and abrupt amplitude differences shown in Figs. 4 (b(vii)), 5 (a(vii)). Results displayed that the signal quality appraisal plays an important role in constructing the dependable heartbeat templates by conserving the actual shapes of the heartbeats. Or else the original shapes of the heartbeat templates can be changed due to the averaging of the noise-free heartbeats with noisy heartbeats which may be included in the unverified reference heartbeat database formation throughout the training phase. Or else, the noisy features may be amassed in the case of ECG waveform features based heartbeat categorization methods. Additional, the SQA based heartbeat categorization method can able of reducing the false alarm rates and misclassification of the noisy heartbeats which are inescapable in many practical ECG recording situation

Table .2 Accomplishment of the ECG-SQA Approaches

Approach	TS	Clean	Noisy	TP	TN	FP	FN	Set(%)	Spt(%)	OA(%)
Ref. [30]	3000	858	2142	1445	554	304	697	67.46	64.57	66.63
Ref. [33]	3000	858	2142	1573	756	102	569	73.44	88.11	77.63
Ref. [35]	3000	858	2142	1489	651	207	653	69.51	75.87	71.33
Our (MITADB)	3000	858	2142	2121	843	15	21	99.02	98.25	98.80

Algorithm 2: Proposed Quality-Aware Heartbeat Classification Method

Input: $F_s = 360$ Hz, $N = 10 * F_s$.

$x[n]$, $n = 1, 2, \dots, N \leftarrow$ Input signal; $F_s \leftarrow$ Sampling frequency

ECG signal quality assessment:

Step0: decay the signal into modes or IMFs

[IMF Residue] = Modified CEEMD(x)

Step1: Obtain HF signal and BW signal

$$BW = \text{Residue}; h[n] = \sum_{i=1}^3 IMF_i[n]$$

Step2: recognition of ECG signal quality

Unacceptable: if $((\max(|BW_k[n]|)) > 0.1)$

$Q = \{ (HF \text{ Noise} = \text{YES} \&\& \max(|h_k[n]|) > 0.1)$

Acceptable: Otherwise

where, $BW_k[n]$ and $h_k[n]$ are the k th block of BW signal and HF signal $h[n]$ respectively.

Candidate ECG signal reformation for acceptable quality:

Step0: Obtain the reconstructed ECG signal as

$$y[n] = \sum_{k=4}^I IMF_k[n]$$

Step1: Obtain candidate ECG signal by adding HF component of QRS complex signal ($q_{HF}[n]$) (obtained from eqn. (4)) and $y[n]$

$$z[n] = y[n] + q_{HF}[n] // \text{Candidate ECG signal}$$

Beat classification:

Step0: Extract all the ECG beats using detected R-peaks using Algorithm 1

Step1: Recognize the extracted ECG beat by computing similarity using (6) with the stored template T_p and RR interval variation

which are inevitable in many realistic ECG recording situations.

3. Proposed method

In this proposed methodology we use CNN classifier for ecg classification and compare with SQA classifier.

Convolutional Neural Network is a deep learning algorithm that shows great capability in image classification. CNN extract features of images by convolution and use the features to classify objects. It is designed to automatically and adaptively learn spatial hierarchies of features [17] through training. An image can be classified when the features vote for the most possible class that the image belongs to.

Deep learning algorithms are deployed to two phases, one is training and another is inference. As a supervised learning algorithm, CNN uses a set of labelled images to train the network. Training process implements back propagation algorithm that updates the parameters in CNN. After the model has been fine-tuned and well trained, the learned model will be used to classify new samples. It is known as inference. The structure and parameters of a neural network is fixed once the training process has done, while inference is implemented every time a new data sample comes.

Therefore, the acceleration of the inference phase is mainly discussed

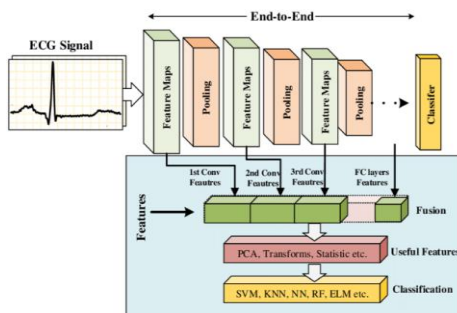


Fig -8: CNN Classifier Technique

3.1 Standard CNN

CNN is structured by layers. In an image classification problem, we expect an image as an input layer and values representing the possibility of different classes as an output layer. Between the input layer and the output layer, there are multiple hidden layers. The hidden layers include convolutional layers, activation function, pooling layers, fully connected layers etc.

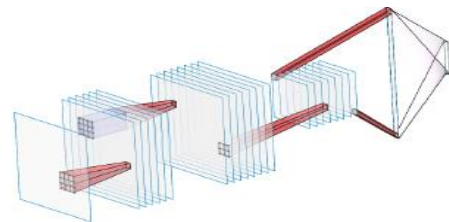


Fig – 9: Structure of Convolutional Neural Network

3.2 Convolutional Layer

A convolutional layer has M input channels and N output channels. Each input channel contains a feature map sized $W_f \cdot H_f$. The $M \cdot W_f \cdot H_f$ input convolves with a convolution kernel sized $M \cdot W_k \cdot H_k$ and produces a $W_f \cdot H_f$ output feature map in one of the output channels. Figure 4.9 shows a convolution with a single kernel. In the convolution kernels are trained weights of the neural network. Convolution with N such kernels produces an output sized $N \cdot W_f \cdot H_f$

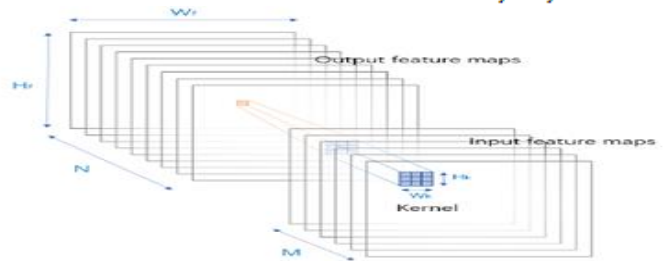


Fig - 9: Structure of Standard Convolutional Layer

W_f is the feature map width, and H_f is the feature map height. W_k is the kernel width, and H_k is the kernel height. For each pixel in input C and output G , the expression is shown in Equation 7, where K represents the convolution kernel.

$$G[n, x, y] = \sum_{i=-\frac{W_k}{2}}^{\frac{W_k}{2}} \sum_{j=-\frac{H_k}{2}}^{\frac{H_k}{2}} \sum_{m=0}^{M-1} C[m, x+i, y+j] \cdot K[n, i, j] \tag{7}$$

3.2 Fully connected layer

In a fully connected layer, the feature map of the preceding layer is flattened to linear structure. Each unit in the feature map acts as a neuron and has full connections to all neurons in the next layer. In a fully connected layer with M input neurons and N output neurons. For each neuron in input X and output Y , the expression is shown in Equation 8, where

W represents the weight of each connection, and B represents the bias of each output neuron.

$$Y[n] = \sum_{m=0}^{M-1} X[m] \cdot W[m, n] + B[n] \quad (8)$$

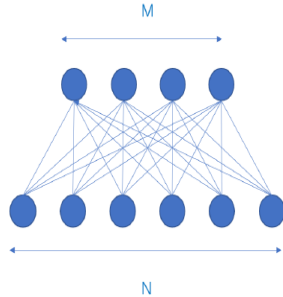


Fig - 10: Structure of Fully Connected Layer

4. RESULTS AND DISCUSSION

The performances are estimated on several normal and abnormal ECG signals taken from 48 recordings of the MITBIH arrhythmia database which includes normal beat (N), premature ventricular contraction (PVC), atrial premature contraction (APC), left bundle branch block (LBBB), right bundle branch block (RBBB), paced beat (P), ventricular fibrillation (VF), fusion of ventricular and normal beat (F), nodal escape (functional) beat (j), fusion of paced and normal beat (f), non-conducted P-wave (x) and unclassified beat (Q) and different kinds of artefacts and noises. The ECG signals were digitized with a sampling rate of 360 Hz and 11-bit resolution over 10 mV range [47]. In this study, the noisy ECG signals are obtained by adding the electrode motion and muscle artifacts which are provided in the ECG noise generator database as mentioned in Ref. [46]. The benchmark measures such as sensitivity (Se), specificity (Sp), positive predictivity (Pp), and overall accuracy (OA) for evaluating the performance of the ECG-SQA approaches that are computed from the true positives (TP), true negatives (TN), false positives (FP), and false negatives (FN) which are obtained for each of test ECG recordings [25], [30], [33], [35]. The categorization accuracy (CA), F1-score, and Kappa measures are used for assessing the performance of the heartbeat classification methods with and without signal quality assessment approach.

4.1 Performance of ECG-SQA Approaches

The presentation of the proposed ECG-SQA move toward and the SQA approaches reported in [30], [33], and [35]. The anticipated SQA achieves the highest overall accuracy of 98.80% with Se of 99.02% and Sp of 98.25%. The anticipated approach offers good false alarm reduction as compared to the other move toward and does not use ECG fiducially features which may not be discriminative and dependable features for assessing the quality of the ECG signals. In this study, the SQA classifies the recorded ECG signals into “acceptable” and “unacceptable”. The acceptable ECG signal segment is further processed in the heartbeat classification stage. Otherwise the noisy ECG signal is not processed if it is sensed as the unacceptable excellence.

Table - 3: Without_SQA

REC	Total	TP	FN	FP	Se	Pp	F1
100	2273	2272	0	69	100	97.05	0.99
101	1865	1864	1	124	99.95	93.76	0.97
102	2187	2185	2	74	99.91	96.72	0.98
103	2084	2071	13	55	99.38	97.41	0.98
104	2229	2215	14	457	99.37	82.9	0.90
105	2572	2570	2	678	99.92	79.13	0.88
106	2027	2011	16	74	99.21	96.45	0.98
107	2137	2137	0	111	100	95.06	0.97
108	1763	1744	19	678	98.92	72.01	0.83
109	2532	2523	9	56	99.64	97.82	0.99

4.2 R-Peak Detection With and Without ECG-SQA Approach

In literature, it is noted that most R-peak recognition approach had high false positive finding rate for the severe noisy ECG signals tainted with muscle artifacts. Some of the approaches had better R-peak detection rates for low and medium backdrop noise levels wherein the QRS complexes are important than the background noise. However, correct and reliable removal of the heartbeats and fiducially feature parameters can be the difficult task when the other ECG local waves are hidden in the muscle artifacts. The detection of noise peaks can lead to make usual false alarms which would be very annoying and disturbing. The extracted noisy ECG beat waveforms may be misclassified due to the inexact measurements of the feature parameters at the classification stage. Thus, in the testing phase, the noisy characteristic parameters can enlarge the misclassification rate of the arrhythmias. Therefore, most R-peak detectors employed search-back heuristic rules with sets of amplitude, duration and period thresholds for rejecting the noise peaks. In practice, it may not be suitable due to the time-varying QRS complex morphologies and heart rates. In this study, the SQA is included with a R-peak detection approach. Table 3 précises the performance of the R-peak detection approach using the denoising approach, with and without ECG-SQA approaches. Results show that the anticipated denoising approach can drastically decrease the false positive detection rate without rising the false negatives. The R-peak detector attain the average Se = 99.67%, Pp = 93.10% and F1-score = 0.96, and the average Se = 99.65%, Pp = 98.88% and F1-score = 0.99 without and with denoising approaches, respectively.

With the SQA method, the R-peak finding attains the average Se = 99.86%, Pp = 99.84% and F1-score = 1. From the studies, it is observed that the some of the ECG signals are extremely tainted with backdrop noises having the intersecting spectra with the ECG local waves. Results show that the proposed denoising approach can conserve the shape of the QRS complexes that is significant for improving the accuracy of heartbeat classification

Table – 4: After Denoising

REC	Total	TP_DEN	FN_DEN	FP_DEN	Se_DEN	Pp_DEN	F1_DEN
100	2273	2273	0	0	100	100	1.0
101	1865	1864	1	2	99.95	99.89	1.0
102	2187	2185	2	6	99.91	99.73	1.0
103	2084	2071	13	11	99.38	99.47	0.99
104	2229	2215	18	177	99.19	92.59	0.96
105	2572	2567	5	195	99.81	92.94	0.96
106	2027	2008	19	7	99.06	99.65	0.99
107	2137	2136	1	12	99.95	99.44	1.0
108	1763	1744	19	215	98.92	89.03	0.94
109	2532	2523	9	4	99.64	99.84	1.0

Table –5: After SQA

REC	Total	TP_SQA	FN_SQA	FP_SQA	Se_SQA	Pp_SQA	F1_SQA
100	1198	1198	0	0	100	100	1.0
101	817	817	0	0	100	100	1.0
102	1385	1385	0	0	100	100	1.0
103	1215	1213	2	0	99.84	100	1.0
104	1044	1038	6	3	99.43	99.71	1
105	718	718	0	8	100	98.9	0.99
106	1189	1182	7	0	99.41	100	1.0
107	1178	1178	0	0	100	100	1.0
108	480	475	5	6	98.96	98.75	0.99
109	1655	1655	0	0	100	100	1.0

4.3 Performance of the Heartbeat categorization Methods

In this study, the heartbeat categorization is executed based on the waveform similarity value measured using the normalized cross-correlation (NCC) metric. The collection heartbeat template of the similar heartbeats is created for each of the heartbeat classes. The comparison between a test heartbeat template and the reference ensemble heartbeat templates is computed at the categorization process. Ten-fold cross-validation process is followed by dividing a total numbers of heartbeats into ten disjoint subsets in which all beat classes are considered in each fold. One-fold is used as test dataset as the residual nine-folds are used as guiding a set for constructing the ensemble heartbeat templates for the proposed approach and creating heartbeat feature models for the other approaches. The justification procedure is repeated for ten times. The average performances of the heartbeat classification approaches are summarized in Table 5 in terms of standard benchmark metrics such as class-specific accuracy (CA), F1-score, Kappa statistic (κ) and false alarm reduction (FAR).

The performance of cross-validation is figured using the kappa statistic to calculate the reliability of accuracy for four classes of heartbeats over ten-folds. It is noted that the

CEEMD+NCC, Hermite, Geometric and Wavelet based categorization methods with the SQA approach had the categorization accuracy of 95.07%, 94.55%, 96.98%, and 89.01% with kappa statistic (κ) of 0.98, 0.99, 0.98 and 0.91, correspondingly for the usual beat detection. Results further show that the higher kappa values can be achieved for the categorization accuracies of the quality-aware categorization method which can be consistent than the categorization method without SQA loom in the case of noisy ECG beats. The F1-score can be better from 0.2 to 0.72 and 0.32 to 0.70, respectively for the S and V beat classes of the CEEMD+NCC based method with the SQA approach. The main objective of this study to revealed that the false alarms can be compact by using the SQA algorithm at the pre-processing stage. Table 5 shows that the false alarm decreases performance for each of the methods. Results show that the existed method can achieve FAR ranging from 24% to 93% under noisy ECG recordings. The Convolutional Neural Networks (CNN) classifier and two different pre-processing techniques of the ECG waveform are applied. One of these techniques uses Hermite basis functions expansion whiles the second characterization of the ECG by the cumulants of the second, third, and fourth orders. The CNN categorization achieves better performance match up to existing technique.

Table – 6: Performance of the classification methods

Beat	kap pa	F1	CA	Kap pa_S QA	F1_S QA	CA_SQA	kap pa_C NN	F1_CNN	CA_CNN	FAR
N	0.78	0.85	74.5 3	0.98	0.97	95.0 7	0.98 7	0.98 8	97.2	96.9
S	0.74	0.2	10.9 9	0.93	0.72	55.7 4	0.95 3	0.78 4	65.8 3	91.3 4
V	0.47	0.32	19.1 1	0.66	0.7	53.9 4	0.79 1	0.79 1	63.2	67.4 1
P	0.72	0.78	64.6	0.88	0.93	87.5 1	0.93 3	0.96 6	92.9	86.6

5. CONCLUSION

In this development, we present a new quality-aware ECG beat classification method which can be capable of reducing the false alarms and ensuring the reliability of set precise accuracies for the four classes of heartbeats in noisy ECG recordings. Assessment results on the standard MIT-BIH arrhythmia database display that the conservation of QRS complexes is most vital for improving the beat classification while the denoising procedure is useful for repression of backdrop noises. The R-peak recognition approach achieves the average Se = 99.67% and Pp = 93.10% and the average Se = 99.65% and Pp = 98.88%, without and with denoising approaches, respectively. With the SQA approach, the R-peak detector achieves the average Se = 99.86% and Pp = 99.84%. Convolutional Neural Network classification results show that the proposed quality-aware heartbeat classification method improves the consistency with improved classification accuracy and F1-score. For each of heartbeat classes, the proposed and existing heartbeat classification

methods had significant improvement in the false alarm reduction (FAR). Results further demonstrate that a quality-aware ECG analysis system is most essential to ensure the accuracy and reliability of diagnosis of different types of arrhythmias under noisy ECG recording environments. The results prove that CNN categorization performs than the ECG Beat categorization.

REFERENCES

- [1] J. Wannenburg, R. Malekian, and G. P. Hancke, "Wireless capacitive based ECG sensing for feature extraction and mobile health monitoring," *IEEE Sensors J.*, vol. 18, no. 14, pp. 6023–6032, Jul. 2018.
- [2] E. Spanò, S. Di Pascoli, and G. Iannaccone, "Low-power wearable ECG monitoring system for multiple-patient remote monitoring," *IEEE Sensors J.*, vol. 16, no. 13, pp. 5452–5462, Jul. 2016.
- [3] D. Labate, F. L. Foresta, G. Occhiuto, F. C. Morabito, A. Lay-Ekuakille, and P. Vergallo, "Empirical mode decomposition vs. wavelet decomposition for the extraction of respiratory signal from single-channel ECG: A comparison," *IEEE Sensors J.*, vol. 13, no. 7, pp. 2666–2674, Jul. 2013.
- [4] P. D. Chazal, M. O'Dwyer, and R. B. Reilly, "Automatic classification of heartbeats using ECG morphology and heartbeat interval features," *IEEE Trans. Biomed. Eng.*, vol. 51, no. 7, pp. 1196–1206, Jul. 2004.
- [5] P. D. Chazal and R. B. Reilly, "A patient-adapting heartbeat classifier using ECG morphology and heartbeat interval feature," *IEEE Trans. Biomed. Eng.*, vol. 53, no. 12, pp. 2535–2543, Dec. 2006.
- [6] T. Mar, S. Zaunseder, J. P. Martínez, M. Llamedo, and R. Poll, "Optimization of ECG classification by means of feature selection," *IEEE Trans. Biomed. Eng.*, vol. 58, no. 8, pp. 2168–2177, Aug. 2011.
- [7] C. C. Lin and C. M. Yang, "Heartbeat classification using normalized RR intervals and morphological features," *Math. Problems Eng.*, vol. 2014, May 2014, Art. no. 712474.
- [8] Q. Li, C. Rajagopalan, and G. D. Clifford, "Ventricular fibrillation and tachycardia classification using a machine learning approach," *IEEE Trans. Biomed. Eng.*, vol. 61, no. 6, pp. 1607–1613, Jun. 2014.
- [9] M. K. Das and S. Ari, "Patient-specific ECG beat classification technique," *Healthcare Technol. Lett.*, vol. 1, no. 3, pp. 98–103, 2014.
- [10] J. Kim, S. D. Min, and M. Lee, "An arrhythmia classification algorithm using a dedicated wavelet adapted to different subjects," *Biomed. Eng. Online*, vol. 10, p. 56, Dec. 2011.
- [11] E. Alickovic and A. Subasi, "Medical decision support system for diagnosis of heart arrhythmia using DWT and random forests classifier," *J. Med. Syst.*, vol. 40, no. 4, pp. 1–12, 2016.
- [12] C. Ye, B. V. K. V. Kumar, and M. T. Coimbra, "Heartbeat classification using morphological and dynamic features of ECG signals," *IEEE Trans. Biomed. Eng.*, vol. 59, no. 10, pp. 2930–2941, Oct. 2012.
- [13] S. Banerjee and M. Mitra, "Application of cross wavelet transform for ECG pattern analysis and classification," *IEEE Trans. Instrum. Meas.*, vol. 63, no. 2, pp. 326–333, Feb. 2014.
- [14] S. Mitra, M. Mitra, and B. B. Chaudhuri, "A rough-set-based inference engine for ECG classification," *IEEE Trans. Instrum. Meas.*, vol. 55, no. 6, pp. 2198–2206, Dec. 2006.
- [15] T. H. Linh, S. Osowski, and M. Stodolski, "On-line heart beat recognition using Hermite polynomials and neuro-fuzzy network," *IEEE Trans. Instrum. Meas.*, vol. 52, no. 4, pp. 1224–1231, Aug. 2003.
- [16] W. Jiang and S. G. Kong, "Block-based neural networks for personalized ECG signal classification," *IEEE Trans. Neural Netw.*, vol. 18, no. 6, pp. 1750–1761, Nov. 2007.
- [17] C. Ye, B. V. K. V. Kumar, and M. T. Coimbra, "An Automatic subject-adaptable heartbeat classifier based on multiview learning," *IEEE J. Biomed. Health Inform.*, vol. 20, no. 6, pp. 1485–1492, Nov. 2016.
- [18] P. Ghorbanian, A. Ghaffari, A. Jalali, and C. Nataraj, "Heart arrhythmia detection using continuous wavelet transform and principal component analysis with neural network classifier," in *Proc. Comput. Cardiology*, Sep. 2010, pp. 669–672.
- [19] K. V. Suarez, J. C. Silva, Y. Berthoumieu, P. Gomis, and M. Najim, "ECG beat detection using a geometrical matching approach," *IEEE Trans. Biomed. Eng.*, vol. 54, no. 4, pp. 641–650, Apr. 2007.
- [20] F. Melgani and Y. Bazi, "Classification of electrocardiogram signals with support vector machines and particle swarm optimization," *IEEE Trans. Inf. Technol. Biomed.*, vol. 12, no. 5, pp. 667–677, Sep. 2008.
- [21] T. Ince, S. Kiranyaz, and M. Gabbouj, "A generic and robust system for automated patient-specific classification of ecg signals," *IEEE Trans. Biomed. Eng.*, vol. 56, no. 5, pp. 1415–1426, May 2009.
- [22] S. Graja and J.-M. Boucher, "Hidden Markov tree model applied to ECG delineation," *IEEE Trans. Instrum. Meas.*, vol. 54, no. 6, pp. 2163–2168, Dec. 2005.
- [23] S. Kiranyaz, T. Ince, and M. Gabbouj, "Real-Time patient-specific ECG classification by 1-D convolutional neural networks," *IEEE Trans. Biomed. Eng.*, vol. 63, no. 3, pp. 664–675, Mar. 2016.
- [24] Y. H. Hu, S. Palreddy, and W. J. Tompkins, "A patient-adaptable ECG beat classifier using a mixture of experts approach," *IEEE Trans. Biomed. Eng.*, vol. 44, no. 9, pp. 891–900, Sep. 1997.
- [25] U. Satija, B. Ramkumar, and M. S. Manikandan, "A simple method for detection and classification of ECG noises for wearable ECG monitoring devices," in *Proc. IEEE Int. Conf. Signal Process. Integr. Netw. (SPIN)*, Feb. 2015, pp. 164–169.
- [26] U. Satija, B. Ramkumar, and M. S. Manikandan, "Robust cardiac event change detection method for long-term healthcare monitoring applications," *IET Healthcare Technol. Lett.*, vol. 3, no. 2, pp. 116–123, 2016.
- [27] E. Morgado et al., "Quality estimation of the electrocardiogram using cross-correlation among leads," *Biomed. Eng. Online*, vol. 14, no. 1, 2015.
- [28] D. P. V. Tobon, T. H. Falk, and M. Maier, "MS-QI: A modulation spectrum-based ECG quality index for telehealth

- applications," *IEEE Trans. Biomed. Eng.*, vol. 63, no. 8, pp. 1613–1622, Aug. 2016.
- [29] Q. Li, R. G. Mark, and G. D. Clifford, "Robust heart rate estimation from multiple asynchronous noisy sources using signal quality indices and a Kalman filter," *Physiol. Meas.*, vol. 29, no. 1, pp. 15–32, Jan. 2008.
- [30] C. Orphanidou, T. Bonnici, P. Charlton, D. Clifton, D. Vallance, and L. Tarassenko, "Signal-quality indices for the electrocardiogram and photoplethysmogram: Derivation and applications to wireless monitoring," *IEEE J. Biomed. Health Informat.*, vol. 19, no. 3, pp. 832–840, May 2015.
- [31] P. X. Quesnel, A. D. C. Chan, and H. Yang, "Real-time biosignal quality analysis of ambulatory ECG for detection of myocardial ischemia," in *Proc. IEEE Int. Symp., Med. Meas. Appl. (MeMeA)*, May 2013, pp. 1–5.
- [32] J. Behar, J. Oster, Q. Li, and G. D. Clifford, "ECG signal quality during arrhythmia and its application to false alarm reduction," *IEEE Trans. Biomed. Eng.*, vol. 60, no. 6, pp. 1660–1666, Jun. 2013.
- [33] G. D. Clifford, J. Behar, Q. Li, and I. Rezek, "Signal quality indices and data fusion for determining clinical acceptability of electrocardiograms," *Physiol. Meas.*, vol. 33, no. 9, pp. 1419–1437, 2012.
- [34] J. Lee, D. D. McManus, S. Merchant, and K. H. Chon, "Automatic motion and noise artifact detection in Holter ECG data using empirical mode decomposition and statistical approaches," *IEEE Trans. Biomed. Eng.*, vol. 59, no. 6, pp. 1499–1506, Jun. 2012.
- [35] D. Hayn, B. Jammerbund, and G. Schreier, "QRS detection based ECG quality assessment," *Physiol. Meas.*, vol. 33, no. 9, pp. 1449–1462, 2012.
- [36] I. Silva, J. Lee, and R. G. Mark, "Signal quality estimation with multichannel adaptive filtering in intensive care settings," *IEEE Trans. Biomed. Eng.*, vol. 59, no. 9, pp. 2476–2485, Sep. 2012.
- [37] I. Jekova, V. Krasteva, I. Christov, and R. Abächerli, "Threshold-based system for noise detection in multilead ECG recordings," *Physiol. Meas.*, vol. 33, no. 9, pp. 1463–1477, Sep. 2012.
- [38] S. J. Redmond, Y. Xie, D. Chang, J. Basilakis, and N. H. Lovell, "Electrocardiogram signal quality measures for unsupervised telehealth environments," *Physiol. Meas.*, vol. 33, no. 9, pp. 1517–1533, Sep. 2012.
- [39] D. Hayn, B. Jammerbund, and G. Schreier, "ECG quality assessment for patient empowerment in mHealth applications," in *Proc. Comput. Cardiol.*, Sep. 2011, pp. 353–356.
- [40] A. C. Maan, E. W van Zwet, S. Man, S. M. M. Oliveira-Martens, M. J. Schaliij, and C. A Swenne, "Assessment of signal quality and electrode placement in ECGs using a reconstruction matrix," in *Proc. Comput. Cardiol.*, Sep. 2011, pp. 289–292.
- [41] K. Noponen, M. Karsikas, S. Tiinanen, J. Kortelainen, H. Huikuri, and T. Seppänen, "Electrocardiogram quality classification based on robust best subsets linear prediction error," in *Proc. Comput. Cardiol.*, Sep. 2011, pp. 365–368.
- [42] B. E. Moody, "Rule-based methods for ECG quality control," in *Proc. Comput. Cardiol.*, pp. 361–363, Sep. 2011.
- [43] U. Satija, B. Ramkumar, and M. S. Manikandan, "A generalized noise detection and classification framework using modified complete EEMD and temporal features for automated ECG analysis," *IEEE J. Biomed. Health Informat.*, vol. 22, no. 3, pp. 722–732, May 2018.
- [44] U. Satija, B. Ramkumar, and M. S. Manikandan, "A unified sparse signal decomposition and reconstruction framework for elimination of muscle artifacts from ECG signal," in *Proc. IEEE Int. Conf. Acoust., Speech Signal Process. (ICASSP)*, Mar. 2016, pp. 779–783.
- [45] P. Kathirvel, M. S. Manikandan, S. R. M. Prasanna, and K. P. Soman, "An efficient R-peak detection based on new nonlinear transformation and first-order Gaussian differentiator," *Cardiovascular Eng. Technol.*, vol. 2, no. 4, pp. 408–425, Dec. 2011.
- [46] P. E. McSharry and G. D. Clifford, "A dynamical model for generating synthetic electrocardiogram signals," *IEEE Trans. Biomed. Eng.*, vol. 50, no. 3, pp. 289–294, Mar. 2003.
- [47] G. B. Moody and R. G. Mark, "The impact of the MIT-BIH arrhythmia database," *IEEE Eng. Med. Biol.*, vol. 20, no. 3, pp. 45–50, May/Jun. 2001.
- [48] M. E. Torres, M. A. Colominas, G. Schlotthauer, and P. Flandrin, "A complete ensemble empirical mode decomposition with adaptive noise," in *Proc. IEEE Int. Conf. Acoust. Speech Signal Process.*, May 2011, pp. 4144–4147.
- [49] Udit Satija, Member, IEEE, Barathram Ramkumar, and M. Sabarimalai Manikandan, Member, IEEE, "A New Automated Signal Quality-Aware ECG Beat Classification Method for Unsupervised ECG Diagnosis Environments", *IEEE SENSORS JOURNAL*, VOL. 19. NO. 1, JANUARY 1, 2019.